Model for line defects in complex-oscillatory spiral waves

Meng Zhan[1,*] and Raymond Kapral[1,†]
[1]*Chemical Physics Theory Group, Department of Chemistry, University of Toronto, Toronto, Ontario, Canada M5S 3H6*
(Received 8 July 2005; revised manuscript received 31 August 2005; published 28 October 2005)

Spiral waves in period-doubled and other complex-oscillatory media possess line defects across which the phase of the oscillation changes by multiples of 2π. For such systems, the concept of a splay state, introduced for coupled oscillator systems, is generalized to an Archimedean spiral splay field. In this splay field a spiral wave in a two dimensional space is considered to be a special splay state where spatial points having identical phase space orbits take phases determined by the Archimedean spiral on which they lie. Using the Archimedean spiral splay field, an equation that determines the shape of the line defect is derived.

DOI: 10.1103/PhysRevE.72.046221 PACS number(s): 05.45.Xt, 89.75.Kd

I. INTRODUCTION

Spiral wave patterns are often observed in excitable and oscillatory media and appear in a variety of physical contexts [1–4]. Early studies of the Belousov-Zhabotinsky (BZ) reaction found spiral wave patterns [5,6]. Spiral waves are frequently observed in surface catalytic oxidation reactions such as CO oxidation on Pt [7]. The aggregation stage of the slime mould dictyostelium discoideum, where the chemical signaling is through periodic waves of cAMP, involves spiral patterns. Spiral Ca^{+2} waves are seen in xenopus laevis oocytes and pancreatic β cells [8]. The appearance and breakup of electrochemical spiral waves are believed to be responsible for various types of cardiac arrhythmias [9].

In oscillatory media, generic features of spiral wave dynamics are usually described in terms of the complex Ginzburg-Landau equation (CGLE), the amplitude equation that is generally applicable in the vicinity of the Hopf bifurcation point [3,4]. However, spiral waves can also exist in complex-oscillatory media where the local dynamics can exhibit period-doubled or even chaotic behavior [10,11]. In such complex-oscillatory regimes, the new feature that appears is the existence of a line defect across which the phase of the oscillation changes by 2π [12,13]. Spiral line defects have been observed and studied experimentally in the BZ reaction under oscillatory conditions [14–17].

Line defects are easily observed in reaction-diffusion systems

$$\partial_t \mathbf{c}(\mathbf{r},t) = \mathbf{R}[\mathbf{c}(\mathbf{r},t)] + \mathbf{D}\nabla^2 \mathbf{c}(\mathbf{r},t), \tag{1}$$

in parameter regimes where the local chemical kinetics, described by the reaction rate $\mathbf{R}[\mathbf{c}(\mathbf{r},t)]$, undergoes a period-doubling bifurcation to chaos. A line defect in the Willamowski-Rössler (WR) reaction-diffusion system [18], with equal diffusion coefficients $D(\mathbf{D}=D\mathbf{I})$ for all species and period-2 local dynamics, is shown in the right panel of Fig. 1. While the local dynamics is period-2 in the bulk of the medium, it is period-1 on the line defect. For comparison, a spiral wave for this system when the local dynamics is period-1 is shown in the left panel of this figure [19].

The WR model involves three chemical concentrations, $\mathbf{c}(\mathbf{r},t)=(c_x,c_y,c_z)$ and the corresponding reaction rates are $R_x=k_1c_x-k_{-1}c_x^2-k_2c_xc_y+k_{-2}c_y^2-k_4c_xc_z+k_{-4}$, $R_y=k_2c_xc_y-k_{-2}c_y^2-k_3c_y+k_{-3}$, and $R_z=-k_4c_xc_z+k_{-4}+k_5c_z-k_{-5}c_z^2$. The visualization of the line defect is achieved by computing the scalar field

$$\Delta c_z(\mathbf{r},t) = \frac{1}{\tau}\int_0^\tau |c_z(\mathbf{r},t+t') - c_z(\mathbf{r},t+\tau+t')|dt' \tag{2}$$

for $\tau=T/2$, where T is the period of the period-2 spiral wave, and converting it to binary form [15]. Since $\mathbf{c}(\mathbf{r},t)=\mathbf{c}(\mathbf{r},t+T/2)$ for the period-1 points on the line defect, while this relation does not apply for other spatial points with period-2 dynamics, the time-average method is easy to implement in order to locate the line defects in the medium.

A line defect is similar to a kink in a bistable system and denotes the location in the medium where the phase of the local oscillation changes rapidly by multiples of 2π due to the broken rotational symmetry. The variation of the concentration field across line defect can be monitored through the computation of a similarity function $S(\xi)$ devised to study phase synchronization [20]. Taking, for instance, the c_z concentration field, we let $c_z^{(2)}$ be the concentration at a point a distance ξ along the normal to the line defect and $c_z^{(1)}$ be the concentration at a far-field reference point sufficiently far from the spiral tip and not near the boundary. The similarity function is defined as following function of the time average of the difference of these concentrations:

$$S_\xi(\tau) = \left(\frac{\langle [c_z^{(2)}(t+\tau) - c_z^{(1)}(t)]^2 \rangle}{[\langle (c_z^{(1)})^2(t)\rangle \langle (c_z^{(2)})^2(t)\rangle]^{1/2}} \right)^{1/2}. \tag{3}$$

Defining $\Gamma(\xi)$ to be the lag time τ corresponding to the minimum of $S_\xi(\tau)$, i.e., $\Pi(\xi)=S(\Gamma(\xi))=\min_\tau S_\xi(\tau)$, we obtain the information needed to describe the behavior in the vicinity of a point on the line defect. As an illustration, Fig. 2(a) plots $\Pi(\xi)$ for $k_2=1.510$. We see that as one moves away from a point on the line defect $\Pi(\xi)$ drops sharply to zero since the dynamics rapidly changes from period-1 to period-2. Thus, the small region (interfacial zone) containing the line defect where the phase rapidly changes by 2π can be determined

*Electronic address: mzhan@chem.utoronto.ca
†Electronic address: rkapral@chem.utoronto.ca

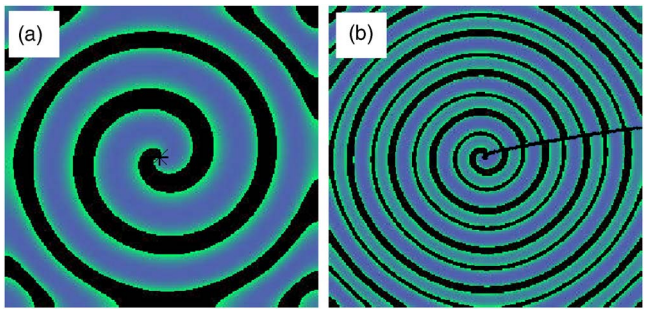

FIG. 1. (Color online) Snapshots of the $c_z(\mathbf{r},t)$ field showing spiral waves in Willamowski-Rössler reaction-diffusion system for two parameter values: $k_2=1.430$ (period-1 regime) (a) and 1.510 (period-2 regime) (b). The other parameters were fixed to be $k_1=31.2, k_{-1}=0.2, k_{-2}=0.1, k_3=10.8, k_{-3}=0.12, k_4=1.02, k_{-4}=0.01, k_5=16.5$, and $k_{-5}=0.5$. (a) There is single defect point (spiral tip), indicated by a large star, for the period-1 spiral wave. (b) The period-2 spiral has a line defect, which is superimposed on the pattern.

from such an analysis. The corresponding time lag $\Gamma(\xi)$ and a quantity $T(\xi)=\|\Gamma(\xi)-\Gamma(-\xi)\|$, where $\|\cdots\|$ denotes the value of the function modulo T, are plotted versus ξ in Fig. 2(b). The period of the oscillation is T. The jumps in these functions across the line defect are evident in the figure.

The spiral waves in the reaction-diffusion systems we consider are Archimedean spirals. In Fig. 3(a) the simulation results in Fig. 1(a) (points) are fit to an Archimedean spiral (thin solid line) using the method described in Ref. [21]. The simulation points are taken from a contour line in the coordinate plane for $c_x=10$ and $c_y>10$, on the upper portion of the Poincare section denoted by a dashed line in Fig. 3(b). Archimedean spirals have been studied experimentally and in models of the BZ reaction [21,22]. The Archimedean structure of the spiral field places strong restrictions on the dynamical behavior and implies a relationship between the geometrical structure in space and the dynamical behavior in time. Using these relationships we show that the form of line defect can be determined.

II. ARCHIMEDEAN SPIRAL SPLAY FIELD

The splay state is a self-organized structure in a spatially-distributed medium in which all local oscillators execute

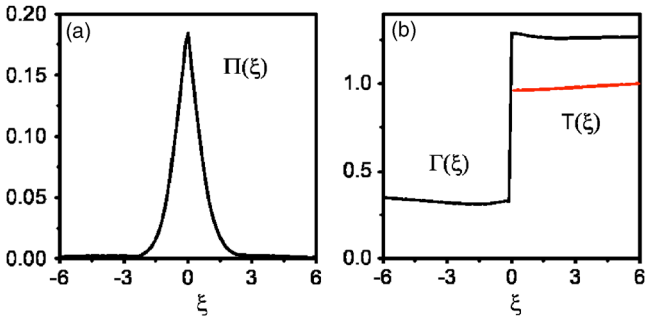

FIG. 2. (Color online) (a) Plot of $\Pi(\xi)$ versus ξ for $k_2=1.510$ locating a point on the line defect and showing the width over which the phase changes rapidly by 2π. (b) Plots of $\Gamma(\xi)$ and $T(\xi)$ versus ξ that appear in the analysis of the similarity function $S_\xi(\tau)$.

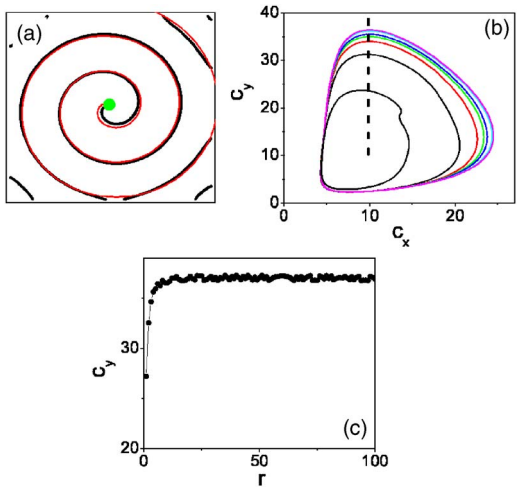

FIG. 3. (Color online) (a) Fit of an Archimedean spiral to the simulation results in Fig. 1(a) at one time instant for $k_2=1.430$. Around the spiral tip, the very small core region is shown as a solid disk. (b) Phase space orbits in the (c_x,c_y) plane, from smallest to largest, are shown at spatial points $r=1$, 2, 3, 4, 5, 10, and 100 along a radius vector, respectively. The dashed line denotes a partial Poincaré section, $c_x=10, c_y>10$. (c) Plot of c_y on the Poincaré section versus the distance r shows that the core region is very small, $r_c\approx 5$ and that the approach to the asymptotic local attractor is rapid.

identical periodic trajectories but with different phases. Such splay states have been extensively investigated in coupled-oscillator systems [23–25]. The phase difference between oscillators can be the same (conventional splay state) [23,24], or functionally controlled (generalized splay state) under weak coupling [25]. Splay states have been observed in physical processes, such as conductance in Josephson-junction arrays [23].

It is well known from studies of the CGLE that the core region that surrounds the topological defect that forms the center of a spiral wave is very small and that outside the core the local dynamics asymptotically tends to a limit cycle attractor with harmonic character [3]. Consequently, the spiral wave may be considered to be a generalized splay state field where the local phase space orbits at all spatial points, except those in the core region, have identical structure but differ in their phases. Similar considerations apply to complex-oscillatory media where the local dynamics has a period-doubled or even chaotic character. In Fig. 3(a), the core region around the spiral tip is indicated by a small disk. The disk diameter is approximately 5, in a pattern with linear a dimension of 256. The local phase space orbits tend to an identical, but not harmonic, local limit cycle attractor as one moves away from the core [see Fig. 3(b)]. In Fig. 3(c) we plot the magnitude of c_y on the Poincaré section [dashed line in Fig. 3(b)] versus the distance r from the spiral tip. The limiting value of c_y is rapidly approached with increasing r. Thus, for such complex-oscillatory spiral wave states we can view the system as being in an Archimedean-spiral generalized splay state with the exception of a small core region.

Given the Archimedean spiral structure, outside the core region, the phase of any point (or the lag time between any

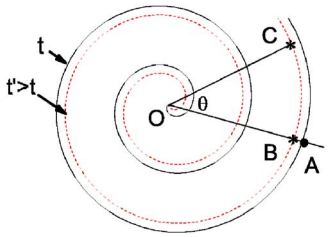

FIG. 4. (Color online) Schematic picture of Archimedean spirals at times t (solid line) and t' (dashed line) with points A,B and C used in the splay field analysis.

two spatial points) can be determined. For instance, an Archimedean spiral (solid line) at time t is shown Fig. 4. A point A on this spiral is given by

$$r_A = \frac{P}{2\pi}(\theta_A - \theta_{A0}), \tag{4}$$

where $P(P=2\pi/\kappa)$ is the pitch, r_A and $\theta_A(+\infty > \theta_A > 0)$ are polar coordinates of point A, and θ_{A0} is the initial angle with respect to a reference axis that characterizes this Archimedean spiral. Counterclockwise is chosen as the positive direction.

Similarly, the point B in this figure lies on another Archimedean spiral (dashed line) at time $t'(t' > t)$ and its equation is

$$r_B = \frac{P}{2\pi}(\theta_B - \theta_{B0}), \tag{5}$$

where $\theta_{B0}(\theta_{B0} \neq \theta_{A0})$ is a different initial phase that characterizes the dashed spiral. Since points A and B lie along the same radial vector they have identical polar angles $(\theta_B = \theta_A)$. We have assumed that the spiral waves are rotating inwardly, which is the most commonly observed case in models of complex oscillatory media [12]. The only difference in the local dynamics between points B and A is the lag time Δt_{BA} that arises from their different initial phases:

$$\Delta t_{BA} = (\theta_{B0} - \theta_{A0})\frac{T}{2\pi} = (r_A - r_B)\frac{T}{P}. \tag{6}$$

More generally, for any point in the domain, say C, which has a polar angle θ that is different from that of A, we can obtain an expression for the lag time between C and A as

$$\Delta t_{CA} = \left[r_A - \left(r_c - \frac{P}{2\pi}\theta\right)\right]\frac{T}{P} = \left[\left(r_A + \frac{P}{2\pi}\theta\right) - r_c\right]\frac{T}{P}, \tag{7}$$

where we have used the fact that C and B have identical phases.

The Archimedean spiral splay field analysis is approximate and will be accurate if the spatial point of interest is outside the core region. Nevertheless, since the core region is small and often we are interested in the dynamical behavior far from this region, the Archimedean splay field model provides a convenient and useful means to describe the structure of spiral waves in complex-oscillatory media. Previously, a simple Archimedean spiral phase matching method was successfully employed to explore the structure of cellular patterns in the 2D CGLE [26].

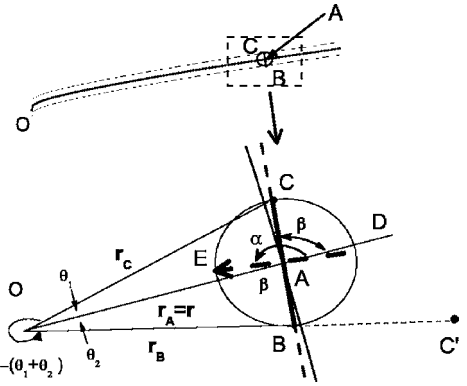

FIG. 5. Schematic picture showing the defect zone surrounding the line defect and the geometry used in the calculation. Upper part: The line defect is denoted by a heavy line and while the zone where the phase changes rapidly is indicated by light solid lines. The region around point A on this line, indicted by a dashed box, is magnified in the lower part of the figure. The perpendicular distance between the two thin lines is 2ξ and $\overline{AB}=\overline{AC}=\xi$. Lower part: In the magnified region in the lower part of the figure, the dashed arrow indicates the tangent direction to the line defect at point A. The angles are $\beta=\angle DAC=\angle BAO$ and $\alpha=\pi/2+\beta=\angle DAE$.

III. LINE DEFECT STRUCTURE

The Archimedean spiral splay field model can be used to construct an equation for the line defect. The top part of Fig. 5 shows a schematic representation of the line defect (heavy solid line) in Fig. 1 for a system with period-2 oscillatory dynamics. At a point A on the line defect, the local dynamics is period-1. In the vicinity of the line defect, there is a narrow interfacial zone, determined by the $\Pi(\xi)$ function plotted in Fig. 2, that connects the period-2 regions on either side of the line that differ in phase by 2π. The two light solid lines on either side of the line defect delimit this zone. Without loss of generality, the two points B and C, as shown in the lower part of Fig. 5, are at the same distance ξ away from the point A. The line BC is perpendicular to the tangent to the line defect at point A, indicated by a dashed arrow. We denote the lengths of the line segments as $\overline{AB}=\overline{AC}=\xi$. A segment of Archimedean spiral curve through A is shown as a thin solid line and the spiral tip, the rotation center, is denoted by O.

On the basis of the Archimedean phase analysis, the lag time $T(\xi)$ between points B and C [note that C is equivalent to point C' under rotation by a counterclockwise angle of $2\pi-(\theta_1+\theta_2)$] is

$$T(\xi) = \left[r_C + P\frac{2\pi - (\theta_1 + \theta_2)}{4\pi} - r_B\right]\frac{T}{P}$$
$$= \left(\frac{1}{2} + \frac{r_C - r_B}{P} - \frac{\theta_1 + \theta_2}{4\pi}\right)T. \tag{8}$$

Points B and C are taken to lie in the period-2 region where

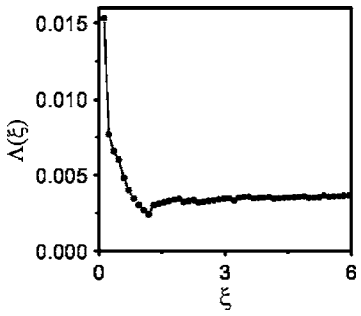

FIG. 6. The determination of the magnitude of Λ through the similarity function computation at $k_2=1.510$. $\Lambda(\xi)=[T(\xi)/T-1/2]/\xi$.

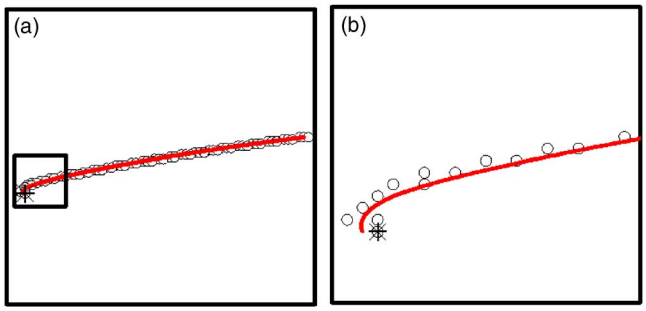

FIG. 7. (Color online) (a) Comparison of the simulation results for the line defect for $k_2=1.510$ (open circles) from Fig. 1(b) with the prediction of Eq. (14) (solid line). (b) A magnification of a portion of the curve in panel (a), indicated by a square, showing the comparison near the spiral tip.

the Archimedean spiral splay field approximation is valid. Assuming that $r_A(r_A=r), r_B, r_C \gg 1$ and $\theta_1, \theta_2 \ll 1$, we have

$$r_C - r_B \approx 2\xi \cos\beta,$$

$$\theta_1 + \theta_2 \approx \frac{2\xi}{r}\sin\beta, \tag{9}$$

where $\beta=\angle DAC=\angle BAO$. Hence, we find

$$T(\xi) = \left(\frac{1}{2} + \frac{2\xi\cos\beta}{P} - \frac{2\xi\sin\beta}{4\pi r}\right)T. \tag{10}$$

Using the fact that the solution X of the equation $a\sin X + b\cos X = c$ where a, b, and c are constants can be written as $\sin(X+\theta)=c(a^2+b^2)^{-1/2}$ and $\theta=\arctan(b/a)$, we obtain

$$\beta = \arctan\left(\frac{4\pi r}{P}\right) - \arcsin\left(\frac{T(\xi)/T - 1/2}{2\xi\sqrt{(1/P)^2 + (1/4\pi r)^2}}\right). \tag{11}$$

From this equation it follows that, $\alpha(r)=\angle DAE$, the angle between the polar and tangent directions of the line defect at A is

$$\alpha(r) = \frac{\pi}{2} + \beta = \frac{\pi}{2} + \alpha_1 - \alpha_2, \tag{12}$$

where

$$\alpha_1 = \arctan\left(\frac{4\pi r}{P}\right),$$

$$\alpha_2 = \arcsin\left(\frac{\Lambda}{2\sqrt{(1/P)^2 + (1/4\pi r)^2}}\right). \tag{13}$$

The equality between α and $\pi/2+\beta$ is independent of shifts in the direction of the line BC around A (clockwise or counterclockwise). In this equation $\Lambda(\xi)$, defined by $\Lambda=[T(\xi)/T-1/2]/\xi$, plays the role of an order parameter. This quantity is plotted in Fig. 6 versus ξ. We see that while $\Lambda(\xi)$ varies rapidly within the interfacial zone surrounding the line defect, it tends to a nearly constant plateau value outside the narrow zone. For the chosen parameters, we find $T=1.919$ and the asymptotic value $\Lambda \approx 0.0036$. Thus, the formula for $\alpha(r)$ is independent of ξ for ξ values outside the interfacial zone.

Given these relations, an equation for the line defect can be constructed. In general, if α is the angle between the polar and the tangent directions of any curve expressed in polar coordinates (r,θ), we have $\tan\alpha = r/r'$, where $r' = dr/d\theta$. Taking the curve to be the line defect we obtain

$$\theta_b = \theta_a + \int_a^b \frac{1}{r}\tan\alpha(r)dr, \tag{14}$$

where θ_a and θ_b are polar angles at two points a and b on the line defect. Thus, given the positions of any point a on the line defect and the spiral tip, we can determine the location of any other point b on the line defect by performing the integral in Eq. (14) using the knowledge of the functional form of $\alpha(r)$.

Qualitative information on the form of the line defect can be deduced from a knowledge of the limiting behavior of $\alpha(r)$ for large and small values of r. As r goes infinity, $\alpha_1(\alpha_2)$ asymptotically approaches $\pi/2\,[\arcsin(\Lambda P/2)]$, and $\alpha(r\to\infty)\approx\pi-\arcsin(\Lambda P/2)$. Note, $\arcsin(\Lambda P/2)\neq 0$ and is small. Thus, it is quite easy to see why the line defect appears to be an approximately straight line whose tangent vector does not point to the spiral tip. As r approaches zero, $\alpha(r\to 0)\approx\pi/2$ as both α_1 and α_2 go to zero. As a result, there will be a large change in the tangent direction for points on the line defect that lie close to the spiral tip.

In Fig. 7(a), the simulation results for the line defect (open circles) are compared with the theoretical prediction of Eq. (14) (solid line) for $k_2=1.510$ where the pitch of the spiral is $P=33.5$ and $\Lambda=0.0036$. Figure 7(b) shows a magnification of the square in Fig. 7(a) [about only one thirty-sixth the size of (a)] and demonstrates that the Archimedean model can predict the structure of the line defect close to the core region.

Thus far we have considered parameter values of the WR model for which the dynamics at spatial points within the defect zone is periodic. As k_2 increases more complicated dynamical behavior is observed [16]. Figure 8(a) for $k_2=1.540$ shows the $c_z(\mathbf{r},t)$ field at one time instant. It has the same apparent spatially period-2 structure as that in Fig.

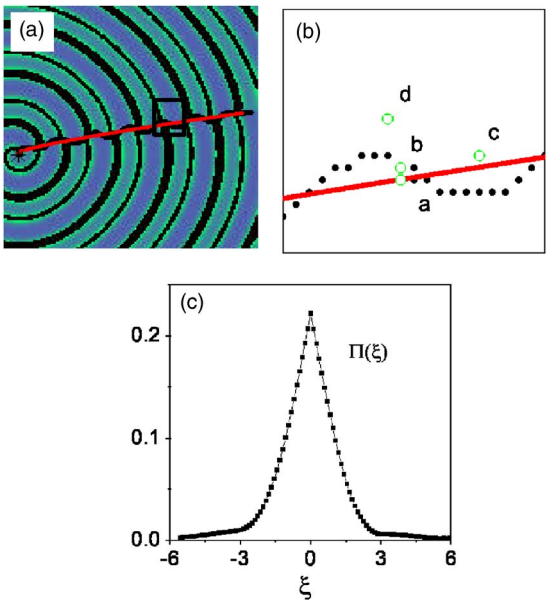

FIG. 8. (Color online) (a) Snapshot of the $c_z(\mathbf{r})$ at one time instant for a larger value $k_2=1.540$ with the so called "wiggling" line with an oscillatory structure and our prediction curve. (b) Four typical points (open circles) around the defect zone are selected to study the dynamics. (c) Plot of $\Pi(\xi)$ versus ξ. Even with the quasiperiodic behavior appearing within the defect region the same defect zone structure as Fig. 2 appears.

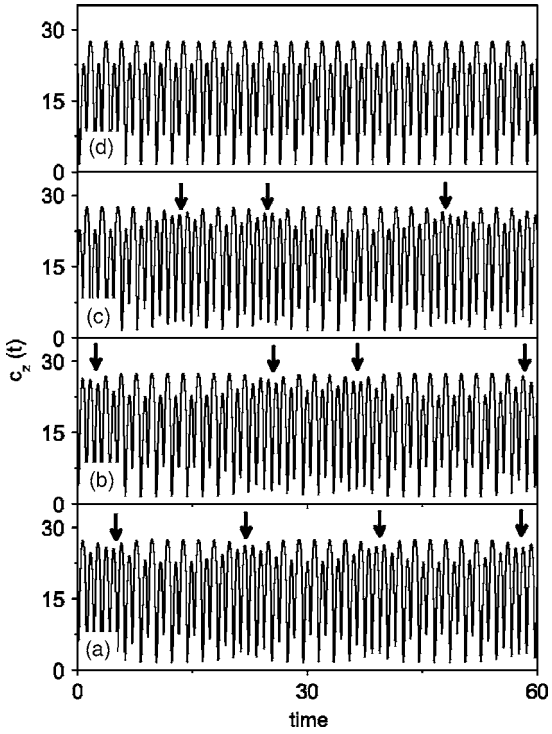

FIG. 9. From bottom to top: Time series $c_z(t)$ of four typical spatial points [see Fig. 8(b)], a, b, c, and d, respectively. Arrows show the positions of local approximately period-1 motions.

1(b) for $k_2=1.510$. Figure 8(c) plots the magnitude of $\Pi(\xi)$ of the similarity function [Eq. (3)], computed from a long time average, versus ξ normal to the defect zone and shows that the defect zone has a structure similar to that depicted in Fig. 2.

A magnification of a small portion of Fig. 8(a) is shown in panel (b) where spatial points a,b,c, and d in the vicinity of the defect region are indicated. The time series at these points are shown in Fig. 9. Points inside the defect zone execute quasiperiodic motion interspersed with short-time segments of approximately period-1 behavior as indicated by the arrows in Figs. 9(a), 9(b), and 9(c). The time interval between two neighboring arrows in the time series is approximately constant for points, like point a, on the theoretical midline of the defect zone [see Fig. 9(a)]. The time interval becomes more irregular, a short (long) segment followed by a long (short) segment, when the spatial point is displaced from the midline [compare Fig. 9(b) with 9(a)]. Points having the same perpendicular distance from the midline have identical orbits but different phases as a comparison of Figs. 9(b) and 9(c) shows. Outside of the defect zone, period-2 behavior is observed [Fig. 9(d)].

In this quasiperiodic regime for $k_2=1.540$, the time-average method described in the Introduction [Eq. (2)] yields a "wiggly" line defect with regular sinusoidal modulation [16]. However, points on the wiggly defect line no longer have identical local dynamics similar to that for the simple curved line defect observed at smaller k_2. The method simply finds the positions of the approximately period-1 time slices in the time series, indicated by the arrows in Fig. 9. The line defect is best represented as a defect zone, within which there is complex quasiperiodic temporal dynamics, which separates simple period-2 behavior with a 2π phase shift across the defect zone. Equation (14) predicts the mean position of the defect zone which is shown as the simple curve in Figs. 8(a) and 8(b) with $P=27.3$ and $\Lambda=0.0029$. Our theoretical description of the line defect shape remains valid for the mean location of this defect zone, since it simply relies on the Archimedean structure of the spiral, which still holds, and the 2π phase jumps across the zone. Note, the core in Fig. 8(a) remains limited to a small region around the tip whose size is not discernibly different from that in Fig. 3(a) at $k=1.430$.

The entire bifurcation structure as a function of k_2 can be summarized as follows. For $k_2<1.530$, the line defect is a simple curve such as that in Fig. 1(b) whose form is predicted by our model and points in the defect zone execute periodic motion. For $1.534<k_2<1.543$ all points in the defect zone execute quasiperiodic motion whose detailed structure was examined in Fig. 9. Our model is able to predict the midline of the defect zone in this case [see Fig. 8(a)]. For $1.530\leqslant k_2\leqslant 1.534$, a hybrid behavior, where periodic behavior far from the spiral tip is combined with quasiperiodic dynamics near the tip, is found. For $k\geqslant 1.543$, chaotic behavior with an irregular character develops within the defect zone.

IV. DISCUSSION

The results presented in this paper show that the Archimedean splay state model can be used to predict the

shape of the line defect in complex-oscillatory domains of model reaction-diffusion systems. However, a number of aspects line defect structure remain to be investigated. A full theoretical description of the line defect structure must be based on a rigorous bifurcation analysis of period-doubling in spiral wave systems and work in this direction is being pursued [27].

In experiments on the Belousov-Zhabotinsky reaction, a number of different line defect structures have been observed. In particular Park and Lee [15] found stationary line defects with spiral and curved shapes and also situations where the core of the spiral to which the line defect is attached executed a meandering motion like that seen in excitable media [2]. These phenomena are richer than those seen in studies of line defects on simple three-variable reaction-diffusion models such as the WR and Rössler models, with one exception. In Ref. [11] a line defect with spiral shape was found for the WR model (see Fig. 8 of this paper) in the regime where the system has locally chaotic dynamics. Due to the large value of the coupling strength $D=100$ used in Ref. [11], in contrast to $D=0.2$ in the present paper, the observed spiral line defect in [11], in fact, lies within the core region. For this system, the spiral line defect may be a spiral core effect and the prediction of its shape is beyond the scope of our model. Our theoretical expression for the line defect shape relies on fairly generic properties, such as the Archimedean nature of the underlying spiral wave and the 2π phase jump across the defect zone. It is able to reproduce the simulation results on model reaction-diffusion systems with period-doubling cascades outside the core region.

Park and Lee [15] also observed that the spiral core begins to move when the period-2 regime is entered. It initially undergoes simple circular motion which develops into "flower" patterns, simlar to those observed in excitable media, as parameters are tuned. Simulations on the Rössler and WR models show a somewhat different behavior [13]. Again, as in the experiments, the core is stationary before entering the period-2 regime and begins to move at the period-2 bifurcation point. However, the motion is ballistic with a very small velocity and the shape of the line defect, which remains at a fixed angle to the direction of the straight-line motion, is constant. Our theory is applicable to this case by working in frame moving with the constant velocity of the spiral point defect at the core. It is possible, as suggested by Park and Lee, that more complex models that incorporate details of the BZ kinetics and reproduce the bifurcations seen in this reacting system need to be constructed to capture these effects. Thus, while our theoretical model for the shape of the line defect does fit the simulation data for the generic WR and Rössler models that show a period-doubling cascade, in the absence of a suitable model that exhibits spiral-shaped line defects, it is not possible for us to investigate their structure.

Guo *et al.* [17] observed that three-dimensional effects can also play a role and lead to new features for both the structure and dynamics of line defects. Such phenomena are outside the scope of our two-dimensional simulations and model theory.

In summary, the Archimedean splay state model can be used to predict shapes of line defects for model reaction-diffusion systems, a feature that was lacking in earlier investigations of these systems. The conditions for the validity of our model are simple and easy to test, and the results accurately describe the simulations on model reaction-diffusion systems exhibiting a period-doubling cascade, although challenges remain for future studies of models with possibly more complex bifurcation structure. The results presented in this paper provide insight into the line defect phenomenon whose study, both experimentally and theoretically, is at an early stage.

ACKNOWLEDGMENTS

We thank S. J Woo and K. J. Lee for providing information on the initial conditions used to produce a clean WR spiral wave. This work was supported in part by a grant from the Natural Sciences and Engineering Council of Canada.

[1] M. Cross and P. Hohenberg, Rev. Mod. Phys. **65**, 851 (1993).
[2] R. Kapral and K. Showalter, *Chemical Waves and Patterns* (Kluwer, Dordrecht, 1995).
[3] I. S. Aranson and L. Kramer, Rev. Mod. Phys. **74**, 99 (2002).
[4] Y. Kuramoto, *Chemical Oscillations, Waves, and Turbulence* (Springer-Verlag, Berlin, 1984).
[5] A. N. Zaikin and A. M. Zhabotinsky, Nature (London) **225**, 535 (1970).
[6] A. T. Winfree, Science **175**, 634 (1972).
[7] G. Ertl, Adv. Catal. **37**, 213 (1990).
[8] A. Goldbeter, *Biochemical Oscillations and Cellular Rhythms* (Cambridge University Press, Cambridge, 1996).
[9] A. T. Winfree, *When Time Breaks Down* (Princeton University Press, Princeton, 1987).
[10] A. Goryachev and R. Kapral, Phys. Rev. Lett. **76**, 1619 (1996).
[11] A. Goryachev and R. Kapral, Phys. Rev. E **54**, 5469 (1996).
[12] A. Goryachev, H. Chate, and R. Kapral, Phys. Rev. Lett. **80**, 873 (1998); A. Goryachev, H. Chate, and R. Kapral, Int. J. Bifurcation Chaos Appl. Sci. Eng. **9**, 2243 (1999).
[13] J. Davidsen, R. Erichsen, R. Kapral, and H. Chate, Phys. Rev. Lett. **93**, 018305 (2004).
[14] J. S. Park and K. J. Lee, Phys. Rev. Lett. **83**, 5393 (1999).
[15] J. S. Park and K. J. Lee, Phys. Rev. Lett. **88**, 224501 (2002).
[16] J. S. Park, S. J. Woo, and K. J. Lee, Phys. Rev. Lett. **93**, 098302 (2004).
[17] H. Guo, L. Li, H. Wang, and Q. Ouyang, Phys. Rev. E **69**, 056203 (2004).
[18] K. D. Willamowski and O. E. Rössler, Z. Naturforsch. A **35**, 317 (1980).
[19] The simulations were performed using the explicit Euler method on a 256×256 square domain with no-flux boundary conditions. The diffusion coefficient was taken to be $D=0.2$. The space and time steps were $\Delta x=1.0$ and $\Delta t=0.001$. To

achieve a perfect WR spiral wave, a special initial condition was used: $D=0.067, \Delta t=0.01$, and $k_2=1.480$ were chosen with two lines of inhomogeneities to induce a rough spiral wave, followed by $D=0.2$ and $\Delta t=0.001$ for larger k_2 to produce clean spirals.

[20] M. G. Rosenblum, A. S. Pikovsky, and J. Kurths, Phys. Rev. Lett. **78**, 4193 (1997).

[21] A. L. Belmonte, Q. Ouyang, and J. M. Flesselles, J. Phys. II **7**, 1425 (1997).

[22] S. C. Muller, T. Plesser, and B. Hess, Physica D **24**, 87 (1987).

[23] K. Wiesenfeld, C. Bracikowski, G. James, and R. Roy, Phys. Rev. Lett. **65**, 1749 (1990); S. Nichols and K. Wiesenfeld, Phys. Rev. E **50**, 205 (1994).

[24] G. Hu, F. G Xie, Z. L. Qu, and P. L. Shi, Commun. Theor. Phys. **31**, 99 (1999).

[25] M. Zhan, G. Hu, Y. Zhang, and D. He, Phys. Rev. Lett. **86**, 1510 (2001).

[26] T. Bohr, G. Huber, and E. Ott, Europhys. Lett. **33**, 589 (1996); Physica D **106**, 95 (1997).

[27] B. Sandstede and A. Scheel, SIAM J. Appl. Dyn. Syst., **3**, 1 (2004).